Phase Synchronization of Nonidentical Light-Sensitive Belousov−Zhabotinsky Systems Induced by Variability in a High−Low Illumination Program

Marc R. Roussel* and Jichang Wang†

Department of Chemistry and Biochemistry, University of Lethbridge, Alberta T1K 3M4 Canada

Received: November 29, 2000; In Final Form: May 29, 2001

Phase synchronization of two systems with different dynamical parameters driven by a common external signal is studied using a model of the photosensitive Belousov−Zhabotinsky reaction. Complex dynamics, including chaos, arise when the external light intensity is periodically switched between two levels. Two dynamical conditions are investigated here: (a) the two systems are driven between two limit cycles and (b) both systems are driven between excitable and oscillatory states. Phase synchronization is achieved with both Gaussian-distributed and dichotomous noise when the random variation is added to the duration of the periodic forcing. In the case that noise is added to the intensity of the periodic forcing, perfect phase synchronization is achieved with dichotomous noise, whereas only transient synchronization is observed with Gaussian-distributed random variation. Studies with correlated noise show that the compound system may have two attractors, one corresponding to the phase synchronized state and one to unsynchronized oscillations (lag-synchronized or chaotic, depending on the parameters). This suggests that transient synchronization is due to noise-induced transitions between the synchronized attractor and the neighborhood of a second invariant set which may in some cases also be an attractor. The synchronization mechanism is also studied using a return map.

1. Introduction

Synchronization phenomena have been studied in various fields such as biology,[1−10] physics,[11−17] and chemistry,[18,19] as well as in a variety of technological contexts.[20] In the case of strong coupling, the motions in different subsystems can completely mimic each other. To realize the synchronization of two systems, one system can be used as a driving force to drive the other (master−slave synchronization)[21] or the two systems can be mutually coupled (bidirectional).[22] Recently, it has been shown that if the synchronized systems have identical dynamics then there is no essential difference between unidirectional and bidirectional coupling.[23] Using an external signal to drive the two systems has also been investigated actively in recent studies.[1,11,18,24] The external signal can be periodic, chaotic or random.[18] Synchronization can sometimes be observed in driven dynamical systems even in the absence of coupling.[1]

In the past decade, methods for synchronizing chaotic systems have attracted increasing interest, prompted by potential applications in secure communication[12] and by research in neuroscience, among other fields.[2] For systems with different structures or parameters, general definitions of synchrony have been developed which do not require the two systems to behave identically.[25] In this study, we investigate phase synchronization of two photosensitive Belousov−Zhabotinsky (BZ) reactions subjected to a common square-wave light perturbation. Phase synchronization is obtained when appropriate variables in two systems reach their maxima or minima with negligible phase delay. The amplitudes may on the other hand remain noncorrelated. Chemical reactions driven by a periodic perturbation have been the subject of many experimental and computational studies in the past 30 years.[26−45] A number of studies on periodically driven chemical reactions have reported the observation of entrainment and consecutive bifurcations leading to chaos.[34−40] Our recent study of the light-sensitive BZ reaction with periodic and nearly periodic switching illustrates that not only are the forcing frequency and amplitude important but that the detailed waveform of the external forcing is also essential in determining the behavior of a driven dynamical system.[19] The addition of random variations to the *durations* of external forcing pulses can synchronize two otherwise chaotic systems which have the same dynamics.

Here we extend our earlier work to explore the feasibility of using random variation to synchronize two systems with different dynamics, oscillating at different amplitudes and frequencies. Synchronization in both amplitude and phase of two systems with different dynamics has been reported by Parmananda and Jiang in a modeling study of electrochemical corrosion.[18] They found that when the two response systems are at unequal parameter values and exhibiting different dynamical behavior synchronization is achieved only for forcing including a random element. A recent study on a forced two-variable biological model system also shows that the noisy switching between two states may tame chaotic phenomena and favor synchronization.[1]

The constructive influence of random fluctuations will be characterized in this study in two different ways: (a) the random variation is added to the *intensity* of the external forcing or (b) the random fluctuation is added to the *duration* of the perturbation. We consider both Gaussian-distributed and dichotomous random variation. Moreover, two types of dynamical situations are investigated here: (a) the two systems are driven between two limit cycles or (b) both systems are driven between excitable and oscillatory states. These switching protocols are easily realizable experimentally in a photosensitive reaction.

* To whom correspondence should be addressed. E-mail: roussel@uleth.ca. Fax: +1 403 329 2057.

† E-mail: wangj@cs.uleth.ca.

10.1021/jp004317x CCC: $20.00
Published on Web 07/11/2001

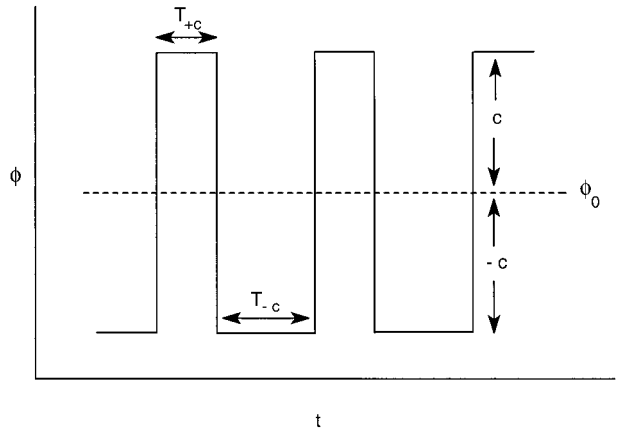

Figure 1. Schematic drawing of the periodic forcing used in this study. ϕ_0 is the bromide production at an average light intensity. The light intensity is varied periodically in such a way that the bromide production rises to $\phi_0 + c$ for T_{+c} time units, then falls to $\phi_0 - c$ for T_{-c} time units.

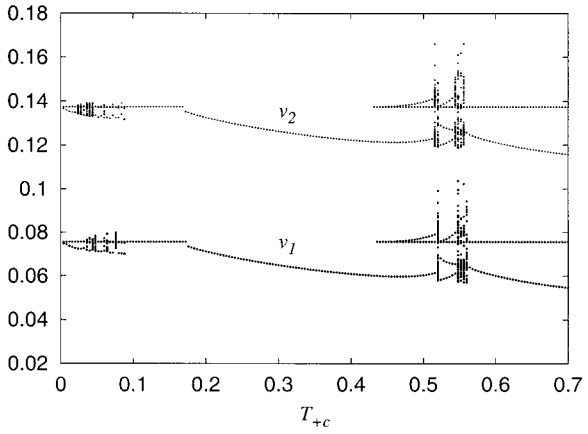

Figure 2. Bifurcation diagrams of the two systems with respect to the variation of T_{+c} while T_{-c} remains constant at 1.1. Other parameter values are given in the text. Points plotted here are the minimum value of v during its time evolution. The value of v_2 is offset by 0.06.

2. Model

As in our previous study,[19] the model adopted here is a two-variable Oregonator,[46] modified to describe the photosensitive BZ reaction[47,48] (the oxidation and bromination of malonic acid by acidic bromate in the presence of metal catalyst $Ru(bpy)_3^{2+}$). The dimensionless form of the model using Tyson-Fife[49] scaling is

$$\epsilon_i \frac{du_i}{dt} = \frac{(f_i v_i + \phi)(q_i - u_i)}{(q_i + u_i)} + u_i(1 - u_i) \quad (1)$$

$$\frac{dv_i}{dt} = u_i - v_i \quad (2)$$

We will consider the case of two uncoupled copies of this system, i.e., $i = 1$ and 2. Here u_i and v_i are respectively the dimensionless concentrations of $HBrO_2$ and $Ru(bpy)_3^{3+}$, f_i is an adjustable stoichiometric parameter, ϵ_i and q_i are scaling parameters, and ϕ represents the rate of bromide production due to irradiation. This rate is proportional to the applied light intensity.[50−55] We decompose the photochemically induced bromide production into $\phi = \phi_0 + \phi_p + \xi$, where ϕ_0 represents production at a background light intensity, ϕ_p represents an applied perturbation, and ξ is a realization of a noise process (Gaussian-distributed or dichotomous) with zero mean value. When studying the effect of random variation in the duration of the periodic forcing, we omit ξ.

We consider a square-wave perturbation, i.e., $\phi_p = \pm c$, where c is an adjustable constant. The durations of the positive and negative perturbations are respectively T_{-c} and T_{+c} (see Figure 1). When studying the effect of random variation in the *duration* of the periodic forcing, $T_{+c} = \bar{T}_+ + \mu$ and $T_{-c} = \bar{T}_- + \mu$, where $\bar{T}_+$ and $\bar{T}_-$ are preselected values of the durations of the periodic forcing and μ is the (white or dichotomous) noise with zero mean. As shown in an earlier study T_{+c} and T_{-c} can each be used as a bifurcation control parameter.[19] Their values in this study are selected in such a way that both systems exhibit complex oscillations.

Random fluctuations in this study are generated as follows: When white noise is investigated, Gaussian-distributed random numbers ξ (or μ) with variance κ are generated. κ is called the noise strength in this study. Values outside the range of $\pm 2\kappa$ are rejected to bound the variability of the random numbers. Consequently, the random fluctuation ξ (or μ) varies between 2κ and -2κ with mean value zero. Dichotomous noise is generated by randomly selecting $\xi = 2\kappa$ or $\xi = -2\kappa$ with equal probability, and similarly for μ. In all cases, a new value of the noise process is only generated when ϕ_p switches from high to low or vice versa. These noise processes are thus closely related to periodic dichotomous noise.[56]

3. Results

3.1. Excitable-to-Oscillatory Switching. We first consider the two systems switching between excitable and oscillatory dynamics. The following parameter values are used: For system 1, $\epsilon_1 = 0.022$, $q_1 = 0.022$, and $f_1 = 1$; for system 2, $\epsilon_2 = 0.021$, $q_2 = 0.0223$, and $f_2 = 1$. Here we choose $\phi_0 = 0.07$ and $c = 0.03$. Therefore, ϕ varies between the two levels $\phi = 0.04$ (oscillatory) and $\phi = 0.1$ (excitable). Figure 2 presents the bifurcation diagrams of the two systems under a common periodic forcing, in which T_{-c} remains constant at 1.1 (dimensionless time units) and T_{+c} is varied. In the region of small T_{+c}, both systems exhibit complex oscillations with multiple minima within each oscillation cycle. Detailed analysis using stroboscopic plots reveals the development of chaos via quasiperiodic bifurcation in this region.[57] There also exist two more narrow parameter windows of T_{+c} within which both systems display complex dynamical behavior. The sizes and positions of the two windows are sensitive to the values of ϵ_i and q_i. It is necessary to change both parameters in order to maintain overlap between the chaotic windows of the two systems subject to the same periodic forcing. The following studies of synchronization are carried out in the regions of the bifurcation diagram in which both systems exhibit complex oscillations. If at least one of the two systems is chaotic in the absence of noise, sensitive dependence on initial conditions guarantees exponential separation of trajectories. This makes synchronization of motion in this region relatively difficult and thus an excellent test of our methods.

Time series of the two systems calculated at $\bar{T}_- = 1.1$ and $\bar{T}_+ = 0.56$ are shown in Figure 3a. Here Gaussian-distributed random variations are added to the durations T_{-c} ($T_{-c} = \bar{T}_- + \mu$) and T_{+c} ($T_{+c} = \bar{T}_+ + \mu$) with strength $\kappa = 0.2$. The noise is turned on at $t = 200$ (dimensionless time units). Figure 3a shows that, shortly after the random process is turned on, the two systems quickly merge to become indistinguishable on the scale of this time series plot. More detailed examination shows that their oscillation amplitudes are still different. The difference

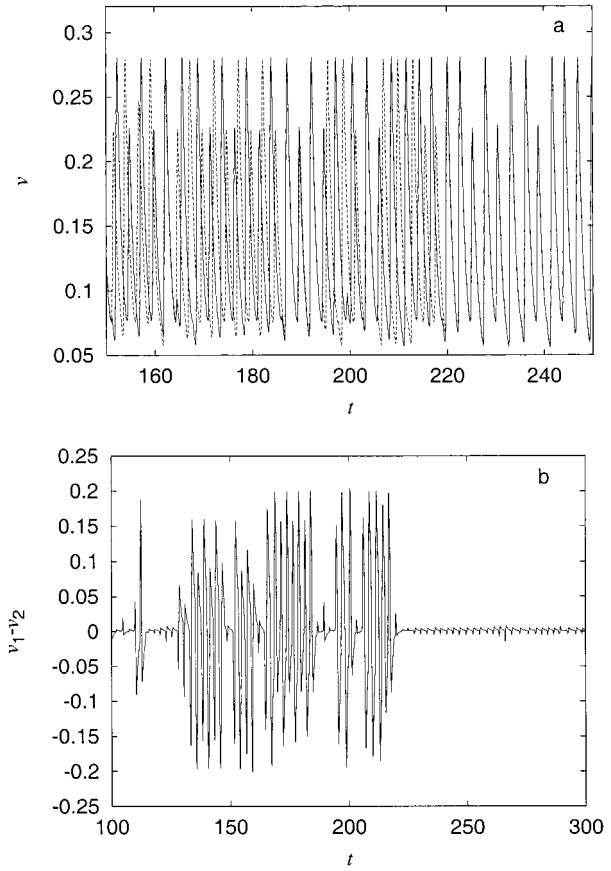

Figure 3. (a) Time series of systems 1 (solid curve) and 2 (dashed line). (b) Time evolution of the difference between these two systems in the variable υ. Gaussian-distributed noise is added to the durations of the forcing (i.e., through μ) and is turned on at $t = 200$. Here $\bar{T}_- = 1.1$, $\bar{T}_+ = 0.56$, and $\kappa = 0.2$. Other parameter values are given in the text.

between the two systems in variable υ is plotted in Figure 3b. As expected, $\upsilon_1 - \upsilon_2$ remains nonzero even after synchronization, so that only phase synchronization is achieved here. Nevertheless, the synchronization is quite impressive. With smaller values of κ, we observed transient synchronization: The synchronized oscillations are frequently interrupted by an unsynchronized state. Calculation of the leading Lyapunov exponent[58] indicates that the two systems are chaotic without noise and then become nonchaotic at sufficiently large noise strengths.

We emphasize here that synchronization is achieved in our model in the absence of coupling between the systems. The only commonality between the two systems is that they receive a common input ϕ. If ϕ is regular, the two systems do not in general synchronize. In the range of parameters considered, the attractor in the (u_i, υ_i, t) phase space can be a limit cycle, a torus, or a chaotic state. In any of these cases, initial phase differences are either maintained (limit cycle and torus) or increased by the dynamics (chaos). However, random variation in the illumination of appropriate strength creates strong correlations between the phases of the driven systems.

Figure 4 presents the results under the influence of dichotomous noise added, again, to the durations of the two phases of the square-wave perturbation. In panel a, we see the projection of a long trajectory onto the (υ_1, υ_2) plane in the absence of noise. The trajectory fills a substantial portion of the accessible part of the plane, indicating an almost complete lack of synchrony. With a noise strength of 0.1 (panel b), the two

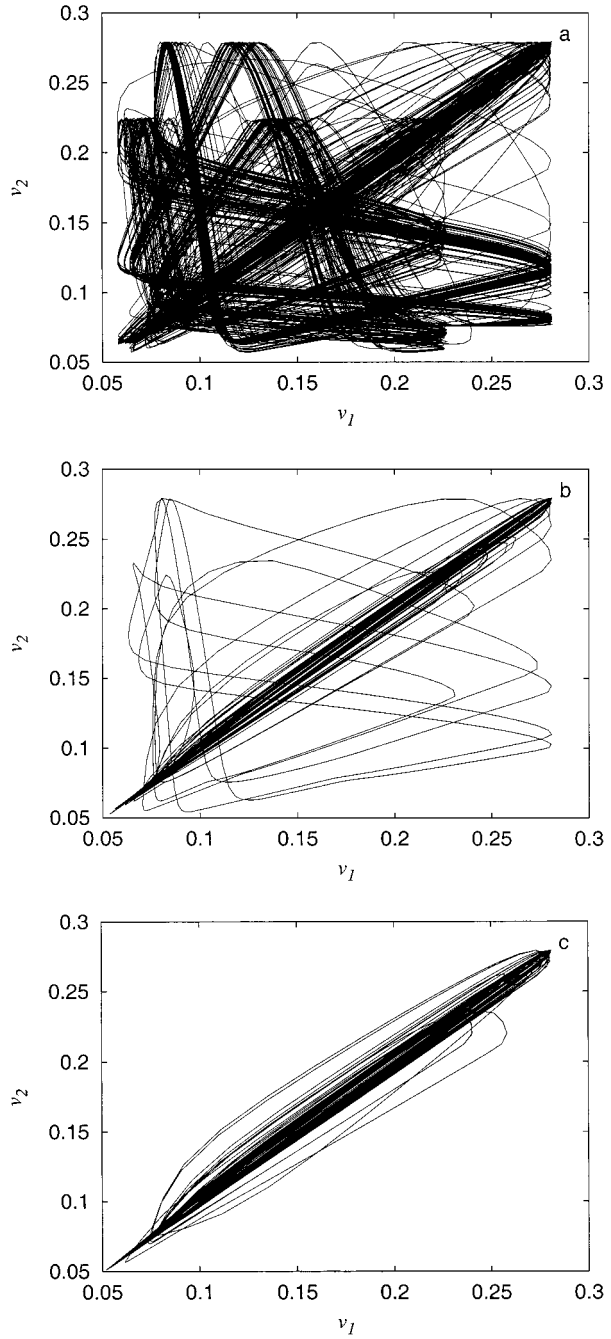

Figure 4. Projections of the dynamics onto the (υ_1, υ_2) plane at different noise levels κ: (a) 0, (b) 0.1, and (c) 0.15. b and c are projections after the achievement of phase synchronization. Here dichotomous noise is applied to the durations of the periodic forcing (i.e., through μ). Other parameter values are the same as those used in Figure 3. In b, we see an example of transient synchronization: The two systems spend most of their time near the line $\upsilon_1 = \upsilon_2$ (representing phase synchronization) with occasional excursions away from this region. At higher noise strengths (c), the trajectories stay in the synchronized state.

systems spend most of their time in the phase synchronized state (near the line $\upsilon_1 = \upsilon_2$) with occasional excursions away from this region. This is an example of transient synchronization. As κ is increased, excursions become less and less frequent. Eventually, phase synchronization between the two systems becomes perfect (panel c). The amplitudes of the oscillations still vary randomly because of the stochastic driving, but the leading Lyapunov exponent is negative. Note that the value of κ required for perfect phase synchronization is smaller with dichotomous noise than it is for Gaussian-distributed noise.

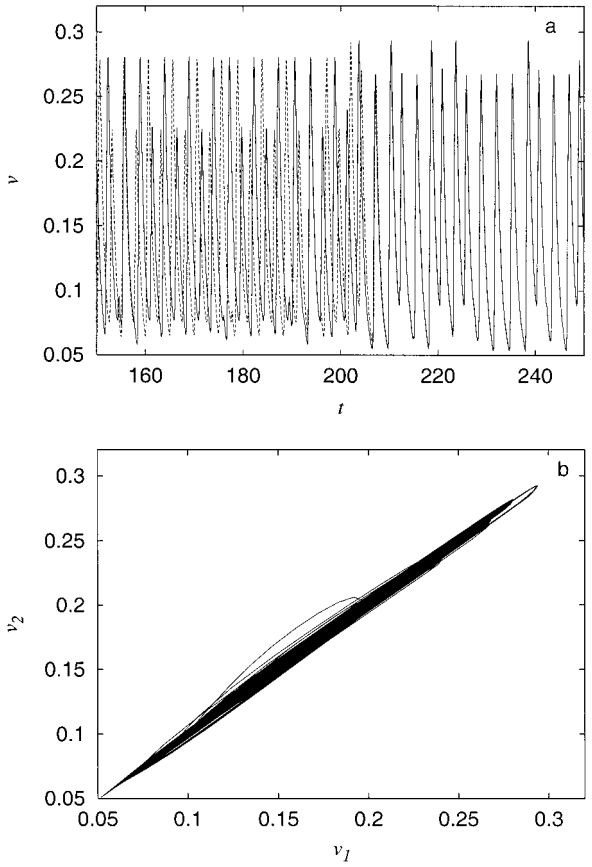

Figure 5. (a) Time series of systems 1 (solid curve) and 2 (dashed line); (b) projection of the dynamics onto the (v_1, v_2) plane after the achievement of phase synchronization. Here dichotomous noise is applied to the intensity ϕ of the periodic forcing (i.e., through ξ) and is switched on at $t = 200$ with noise strength $\kappa = 0.0075$ for $T_{+c} = 0.56$ and $T_{-c} = 1.1$. Other parameter values are given in the text.

The effects of dichotomous noise added to the light intensity ϕ (i.e., through ξ) are presented in Figure 5. The noise strength κ equals 0.0075 in this calculation. Recall that during each period of the forcing, ξ remains constant; that is, a new random intensity is only chosen at switching time. Time series plots in Figure 5a show that the two systems quickly synchronize after turning on the noise at $t = 200$, though the modulation of oscillation amplitudes becomes more pronounced because of the random variation of the light intensity ϕ. Figure 5b shows the relationship between corresponding variables in the concentration space after the achievement of synchronized oscillations. The evolution process of the two systems in the (v_1, v_2) plane before the addition of noise is the same as that shown in Figure 4a. In the presence of dichotomous noise, the complex trajectory illustrated in Figure 4a collapses onto a narrow trajectory, suggesting that the phases are now locked in a more-or-less fixed relationship. When Gaussian-distributed noise is used, qualitatively the same results are obtained. Moreover, transient synchronization is observed when κ takes smaller values, as in the earlier case.

3.2. Oscillatory Systems. Here we choose $\phi_0 = 0.03$ and $c = 0.02$. Therefore, ϕ varies between the two levels, $\phi = 0.05$ and 0.01, which are below the Hopf bifurcation thresholds both of system 1, for which $\epsilon_1 = 0.02$, $q_1 = 0.022$, and $f_1 = 1$, and of system 2, for which $\epsilon_2 = 0.021$, $q_2 = 0.0225$, and $f_2 = 1$. Without periodic switching, both systems exhibit simple limit cycles at $\phi = 0.05$ and at 0.01. Figure 6 presents the bifurcation diagrams of the two systems with respect to the continuous variation of T_{+c}, whereas T_{-c} is kept constant at 1.1. When T_{+c}

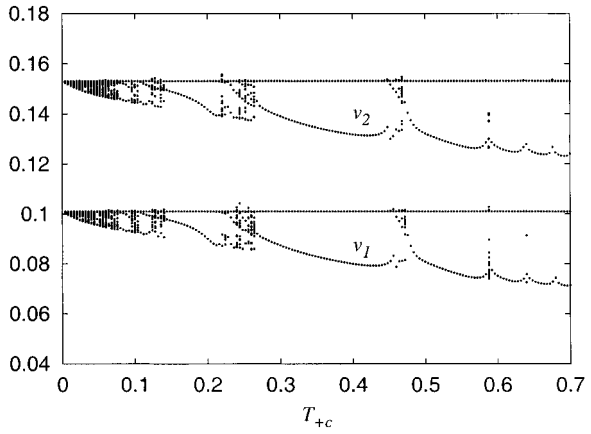

Figure 6. Bifurcation diagrams of the two systems with respect to the variation of T_{+c} while T_{-c} remains constant at 1.1. Other parameter values are given in the text. Points shown here are the minimum values of v during their time evolution. The value of v_2 is shifted up by 0.05.

takes small values (<0.1), both systems exhibit quasiperiodic oscillations and a transition to chaos via quasiperiodic bifurcation. Above $T_{+c} = 0.3$, both systems exhibit complex dynamical behavior only in very narrow ranges.

We first add Gaussian-distributed random fluctuations to the durations of the two phases of the forcing (i.e., through μ). When $\overline{T}_- = 1.1$ and $\overline{T}_+ = 0.243$, the above two systems exhibit chaos, with positive leading Lyapunov exponents ($\lambda_1 = 0.035$). The time evolution of the two systems is presented in Figure 7a, in which the noise was turned on at $t = 200$. After a short transient period, the oscillation phases of the two systems come into correspondence, although their oscillation amplitudes remain different. The relationship between corresponding variables in the concentration space is plotted in Figure 7 parts b and c. In Figure 7b, the evolution process of the two systems covers the full accessible region of the (v_1, v_2) plane, implying that there does not exist a simple functional relationship between their oscillation phases. However, after turning on noise (Figure 7c), this complex trajectory collapses onto a simple narrow one, indicating that their phases are now locked in a more-or-less fixed relationship. When dichotomous noise is added to the duration of the forcing, qualitatively the same results as those shown in Figure 7 are achieved. Again, the required noise strength κ for achieving perfect phase synchronization is smaller than that for Gaussian-distributed random variations.

Figure 8 presents the result when Gaussian-distributed random variations are added to the light intensity ϕ of the periodic forcing. The noise strength κ equals 0.0045 in this calculation. Time series plots in this figure show that the two systems quickly synchronize after turning on noise at $t = 200$, though there is a pronounced modulation of the oscillation amplitudes because of the random variation of the light intensity ϕ. However, the synchronized state is occasionally interrupted by a short period of unsynchronized oscillations. The occurrence of this unsynchronized state becomes less frequent when the noise strength κ is increased. In this case, transient phase synchronization is due to the small noise strength selected because the same phenomenon also occurs when weak noise is applied to the durations of the perturbation. In the version of the model studied here, the maximum noise strength κ is restricted by the background light intensity ϕ_0 and the periodic forcing amplitude c, as the overall value of ϕ must remain above zero. Even with larger values of κ, we are unable to achieve perfect synchronization without any interruption.

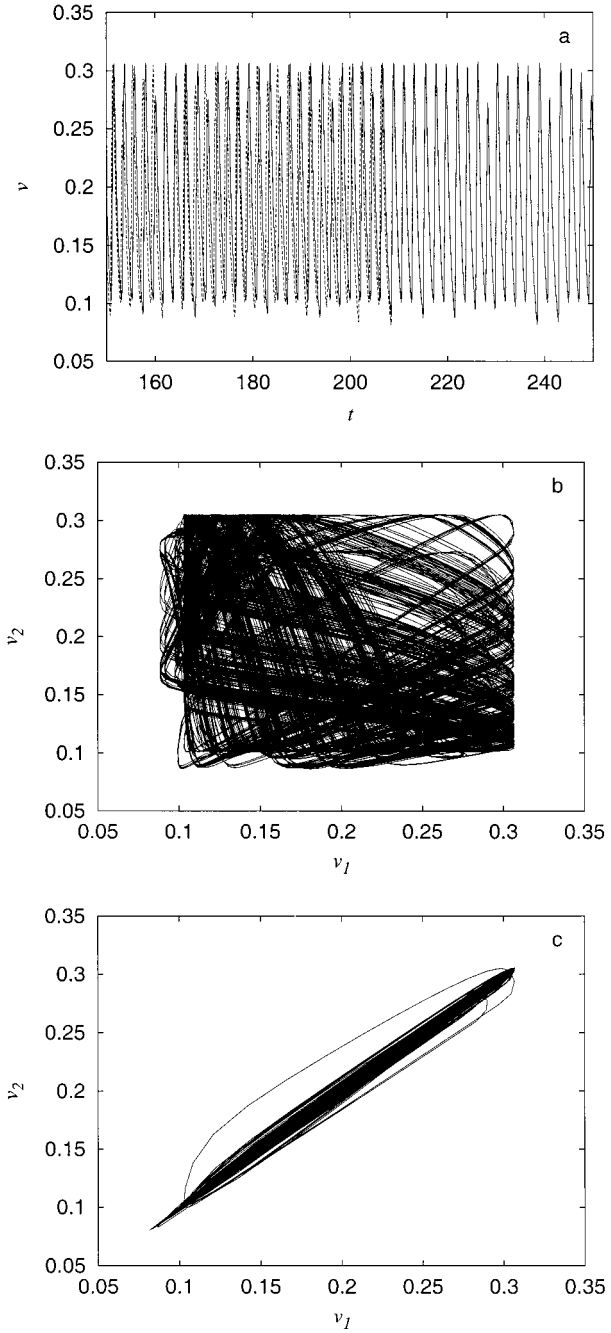

Figure 7. (a) Time series of systems 1 (solid curve) and 2 (dashed line); (b) projection of the dynamics onto the (v_1, v_2) plane in the absence of noise; (c) projection after the achievement of phase synchronization. Here Gaussian-distributed noise is applied to the durations of the two phases of the forcing (i.e., through μ). Noise of strength $\kappa = 0.12$ is turned on at $t = 200$ (dimensionless time units). $\bar{T}_- = 1.1$, $\bar{T}_+ = 0.243$, and other parameter values are given in the text.

Figure 9 shows the results when dichotomous noise is added to the intensity ϕ of the periodic forcing. The plot of corresponding variables in the (v_1, v_2) phase plane suggests that perfect phase synchronization is achieved here. The evolution process of the two systems in the concentration space before the addition of noise is the same as that shown in Figure 7b, covering the full accessible region of the (v_1, v_2) plane.

3.3. Correlated Noise. The noise processes studied thus far are uncorrelated, in the same sense that the velocity in Brownian motion is an uncorrelated random variable: A new value of the appropriate random variable is selected every time the forcing switches from high to low, or vice versa, without regard to earlier values of the random variable. It is natural to wonder what the effects of introducing correlations in successive random trials might be. We have studied these questions briefly. Much of what we have learned simply confirms the general picture developed in earlier sections, although some of our results hint at considerable dynamical richness.

We started with a very simple driving process: We used a copy of our periodically driven system operating in an appropriate parameter range to generate a chaotic signal. We sampled this signal to obtain a sequence of values. A linear transformation was applied to this sequence to generate a sequence of values of μ of appropriate amplitude and zero mean. This process is not random, but a chaotic system does display correlated fluctuations which have some of the properties of noise. The results (not shown) are similar to those obtained with uncorrelated noise. Stable phase synchronization can be achieved provided the sampling time of the chaotic trajectory is not too short. (If the sampling time is too short, then only a small part of the chaotic trajectory is used to generate the fluctuations. Thus, a slowly varying modulation is generated instead of a sequence displaying chaotic fluctuations.)

The chaotic driving described above has rather complex statistical properties. We therefore decided to study the effect of fluctuations whose statistical properties are more easily understood. We chose a two-state Markov chain.[59] Again, the duration of (e.g.) the negative perturbation was computed at the moment of switching by $T_{+c} = \bar{T}_+ + \mu$, where μ is a random variable chosen randomly from the two values $\pm 2\kappa$ at the onset of the perturbation. For simplicity, we can label the two possible values of μ by their signs, "+" and "−". In a Markov chain, the system "remembers" the last choice it made. We then introduce a probability P_{+-} of selecting "−" given that the last choice was "+", and P_{-+} of selecting "+" given that the last choice was "−". The probabilities P_{++} and P_{--} are then fixed by normalization. To make the mean fluctuation zero, we constrain $P_{-+} = P_{+-}$, which in turn implies that $P_{++} = P_{--} = 1 - P_{+-}$. Note that the case $P_{+-} = 0.5$ corresponds to the simple (uncorrelated) dichotomous noise process discussed earlier. We proceeded similarly with the duration of the positive perturbation T_{-c}. Note that the two Markov chains (for each of the two durations) are independent.

We already know the behavior for $P_{+-} = 0.5$: excellent phase synchronization is achieved in this case. Similar results are obtained when P_{+-} is close to 0.5. However, when P_{+-} is made significantly different from 0.5 (i.e., as successive values of μ become either more correlated or anticorrelated), the synchronized oscillations are interrupted by unsynchronized oscillations, similar to the transient synchronization shown in Figure 8. The interruptions occur more and more frequently and last longer as P_{+-} approaches either 0 or 1. At the extremes ($P_{+-} = 0$ or 1 exactly), we are back to periodic forcing. (If $P_{+-} = 1$, this periodic forcing alternates between two durations for each of the positive and negative perturbations.) In some cases, especially if $P_{+-} = 1$, the bias introduced by μ may push the system out of the chaotic regime and allow synchronization. However, even in these cases, the dynamics may be complex. In some cases, there may be two attractors for the composite system, one in which the two reactors are phase synchronized and one in which lag synchronization[25] is observed (i.e., the two reactors repeat the same pattern out of phase). Figure 10 gives an example of these coexisting attractors. The only difference between the two simulations is that the value of the dichotomous noise variable μ was -0.2 when fluctuations were first added

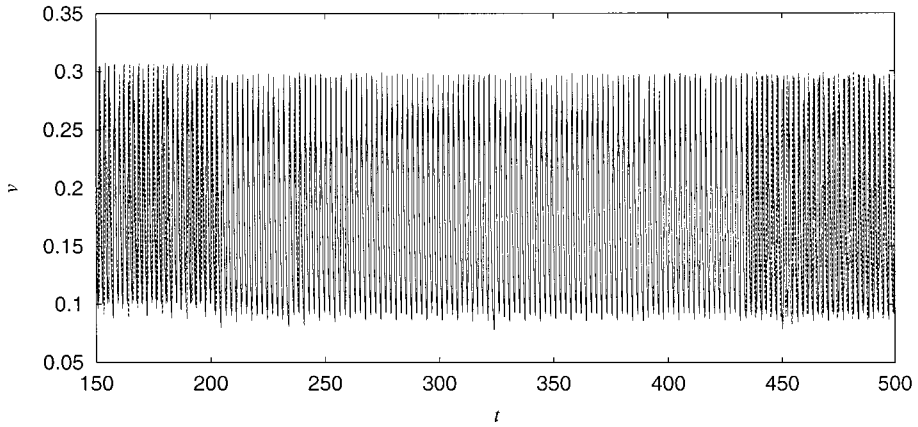

Figure 8. Time series of systems 1 (solid curve) and 2 (dashed line). Gaussian-distributed random variations are added to the intensity ϕ of the periodic forcing (i.e., through ξ). Noise of strength $\kappa = 0.0045$ is switched on at $t = 200$. Other parameter values are the same as those used in Figure 7. Here phase synchronization is occasionally lost.

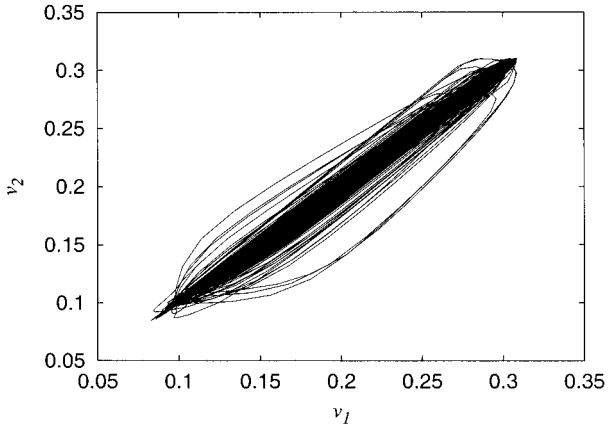

Figure 9. Projection of the dynamics onto the (v_1, v_2) plane after the achievement of phase synchronization. Here dichotomous noise of strength $\kappa = 0.004$ is applied to the intensity ϕ of the periodic forcing (i.e., through ξ). Other parameter values are the same as those employed in Figure 7.

in panel a and +0.2 in panel b. Although this behavior is not universal, we have here one way to understand intermittent synchronization: There are two attractors for the composite system, one of which corresponds to phase synchronization. Under favorable conditions, the composite system spends most of its time near the phase synchronized attractor. However, the random process can cause transitions between this attractor and an unsynchronized (or lag-synchronized) state.

A somewhat similar phenomenon is observed when we try to apply our methods to a nonchaotic driving regime. Figure 11 shows the result of adding Gaussian-distributed noise to the durations of the two phases of the perturbing square wave at values of the parameters which result in regular oscillations. After turning on noise at $t = 200$, the two systems require a rather long transient period (depending on the realization of the noise process and on the noise strength) to achieve a synchronized state. However, the two systems in the same (or nearly the same) locations of the phase space may respond to the same perturbation differently because of the slightly different parameters. When this happens, noise will desynchronize the two synchronized systems, causing flipping between synchronized and unsynchronized states (see Figure 11). Noise thus causes switching between two dynamical states of the compound system, namely, synchronized and unsynchronized (or lag-synchronized) oscillations. The synchronized state is clearly always locally attracting at sufficiently large noise strength. The unsynchronized state may under certain conditions (such as the

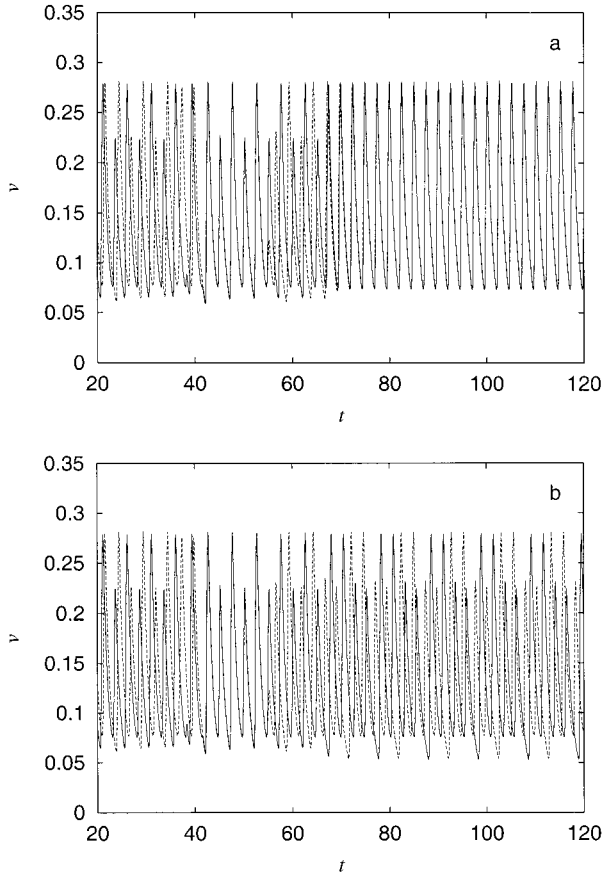

Figure 10. Time series of systems 1 (solid curve) and 2 (dashed line) calculated at different initial values of μ: (a) −0.2 and (b) 0.2. Here dichotomous noise is applied to the durations of the periodic forcing (i.e., through μ) and is turned on at $t = 65$. Other parameter values are the same as those used in Figure 3. The dichotomous "noise" is generated by a Markov process with $P_{+-} = 1$.

case illustrated in Figure 10 and, probably, in the case illustrated in Figure 11) also be an attractor. In other cases, trajectories are simply pushed onto the stable manifold of a repeller before being sent back to the phase-synchronized attractor along the repeller's unstable manifold.

3.4. The Synchronization Mechanism. In an earlier paper, we emphasized that it is necessary to analyze the trajectories in phase space to understand synchronization in these systems.[1] The key concept in this earlier study was a decomposition of phase space into expanding and contracting regions. Although

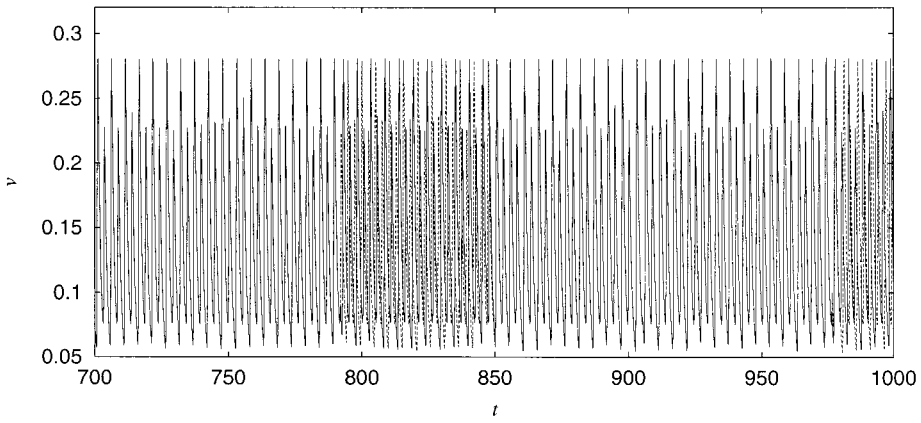

Figure 11. Time series of systems 1 (solid curve) and 2 (dashed line) with $\bar{T}_- = 1.1$ and $\bar{T}_+ = 0.64$. Other parameter values are listed in section 3.1. Here Gaussian-distributed noise is added to the duration of the periodic forcing with noise strength $\kappa = 0.05$. Noise is switched on at $t = 200$.

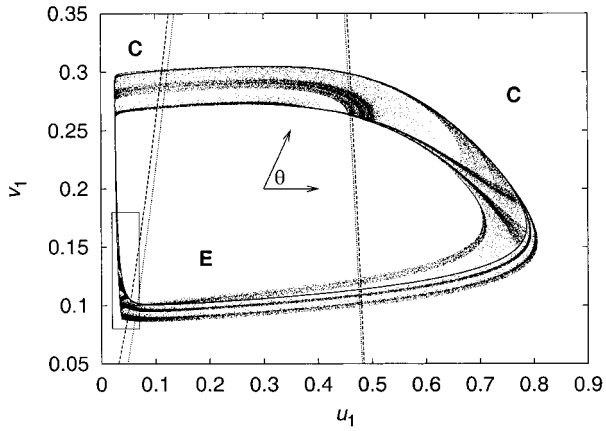

Figure 12. Attractor of system 1 for the parameters of Figure 7 (limit cycle to limit cycle switching) and $\kappa = 0$. The dashed curve is the boundary separating the contracting (C) and expanding (E) regions of phase space for $\phi = 0.01$. The dotted curve is the contracting to expanding boundary for $\phi = 0.05$. Synchronization is associated with switching while both systems are passing through the boxed region, in which the system passes from a strongly contracting to the expanding region of phase space. The figure also shows the definition of the phase angle θ.

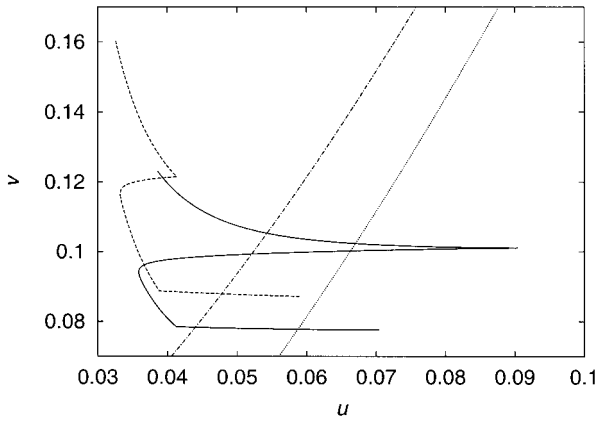

Figure 13. Trajectories experiencing switching events in the boxed region of Figure 12 with parameters set as those in Figure 7, with dichotomous switching of strength $\kappa = 0.12$. The solid curve corresponds to the trajectory for system 1; the dashed curve is for system 2. The photochemical bromide production is switched from the low ($\phi = 0.01$) to the high ($\phi = 0.05$) value, causing the first sharp turn in each of the two trajectories. The boundary of the expanding region simultaneously moves from the dash−dot curve to the dotted curve. (These curves are drawn for the parameters of system 1. The corresponding curves for system 2 are very near those of system 1.) The transients move the two systems deep into the contracting region. In fact, system 1, which was initially out of the contracting region, gets pulled back in by the switching event.

there are some important qualitative differences between the Novak−Tyson cell cycle model and the light-sensitive Oregonator, a similar style of analysis turns out to be helpful here.

In the chaotic regime, the attractors for the switched Oregonators tend to have a similar appearance to that shown in Figure 12. The original periodic orbits of the unswitched systems appear as dark boundary curves in the attractor. The attractor crosses expanding and contracting regions of phase space which can be computed (for each value of ϕ) by finding the curve on which the divergence of the flow velocity $\boldsymbol{v}_i = (\dot{u}_i, \dot{v}_i)$ is zero. For the current model, $\nabla \cdot \boldsymbol{v}_i = 0$ when

$$v_i = \frac{1}{f_i}\left\{\left(\frac{(1 - 2u_i - \epsilon_i)(q_i + u_i)^2}{2q_i}\right) - \phi\right\}$$

These curves are also shown in Figure 12 for the two values of ϕ between which the system is switched.

We noticed (by examining a number of trajectories at different parameter values) that switching events which occurred when the two systems were in the lower left corner of the attractor (boxed in Figure 12) tended to synchronize the two systems. Even when trajectories start out far apart, they will eventually transiently drift into phase, whether their parameters are identical or not. In the former case, the drift is due to different effect of switching in different regions of the attractor, sometimes slowing and sometimes accelerating angular motion around the attractor. If the parameters are different, the parameter difference also causes phase drift because of the different periods of the two oscillators. Figure 13 shows a detail of two trajectories which experience a synchronizing switching event as they pass through the boxed region in Figure 12. The two systems are initially relatively far apart. Switching drives both systems deeper into the region in which strong contraction occurs. (In fact, system 1 is initially outside the contracting region and gets driven back in by the switching event.) Note that, because the parameters are similar, all aspects of the overall dynamics (shape of attractor, boundaries of contracting region, etc.) are similar for the two systems. As a result of undergoing a relatively long stay in the contracting region, the two systems are much more nearly synchronized on exit from this region than they were before switching.

To simplify the dynamics, we define a phase angle θ as shown in Figure 12. Figure 14 shows the Euclidean distance between the same two trajectories as those in Figure 13 plotted against

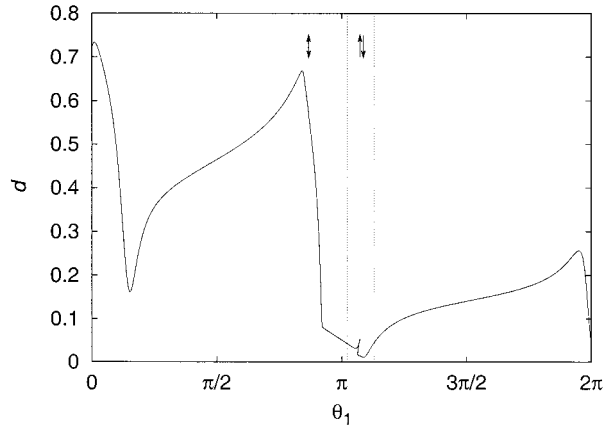

Figure 14. Euclidean distance between the two systems in phase space (d) vs phase angle of system 1 (θ_1) for the same realization of the noise process as in Figure 13. The expanding and contracting regions of phase space can clearly be seen in this graph as regions of positive and negative slope, respectively. Switching events are denoted by arrows. The first pair of switching events is very short and occurs in the wrong region of phase space to have much effect on the dynamics. The second shift up in ϕ (an alternative view of which is shown in Figure 13) forestalls reinjection of the trajectories into the expanding region and leads to a sharp decrease in d. The dotted lines delimit the region in which switching events tend to be particularly effective for synchronization (the boxed region of Figure 12).

the phase angle of system 1 for a full circuit around the attractor. Passage of the two systems through expanding and contracting regions of phase space appear respectively as regions of positive and negative slope in this figure. The second switch from low to high ϕ in Figure 14 (corresponding to the sharp cusp in the trajectory segments in Figure 13) interrupts the increase in d and in fact causes a sharp decrease in this statistic. Repeated events of this nature eventually cause synchronization. Note that similar events occurring at angles near the first minimum in the $d(\theta_1)$ curve can also contribute to synchronization but are much less important for two reasons: First, this minimum is much more narrow than the second one, which means that the window of angles at which switching will assist synchronization is much smaller in the region of the first minimum. Second, the divergence is much less negative in the region of the first minimum than it is near the second, meaning that the contraction in the former region is much weaker.

In the chaotic (small κ) case, these synchronizing events still occur, as it will happen from time to time that both systems pass through the appropriate region simultaneously and experience a switching event there. However, the pattern of switching events is such that it is likely that the two systems will subsequently wander away from each other. Clearly, noise in the switching times alters this pattern in some significant way. To understand this further, we construct a Poincaré map by recording the phase angles θ_i at which switching from the low to the high value of ϕ occurs over a long trajectory. Then we construct a return map by plotting θ_{i+1} vs θ_i. Figure 15 shows return maps for the purely deterministic system ($\kappa = 0$) as well as for systems in which the switching times are subjected to dichotomous or Gaussian noise. The map corresponding to the deterministic system (panel a) has some steeply sloped sections which are responsible for the chaotic behavior because small differences in θ_i result in large differences in θ_{i+1}. Moreover, trajectories which pass through the synchronizing region (the box in Figure 12, corresponding to the phase angles delimited by dotted lines in Figure 15) always take at least two steps of the map before returning to this region. As we increase the noise

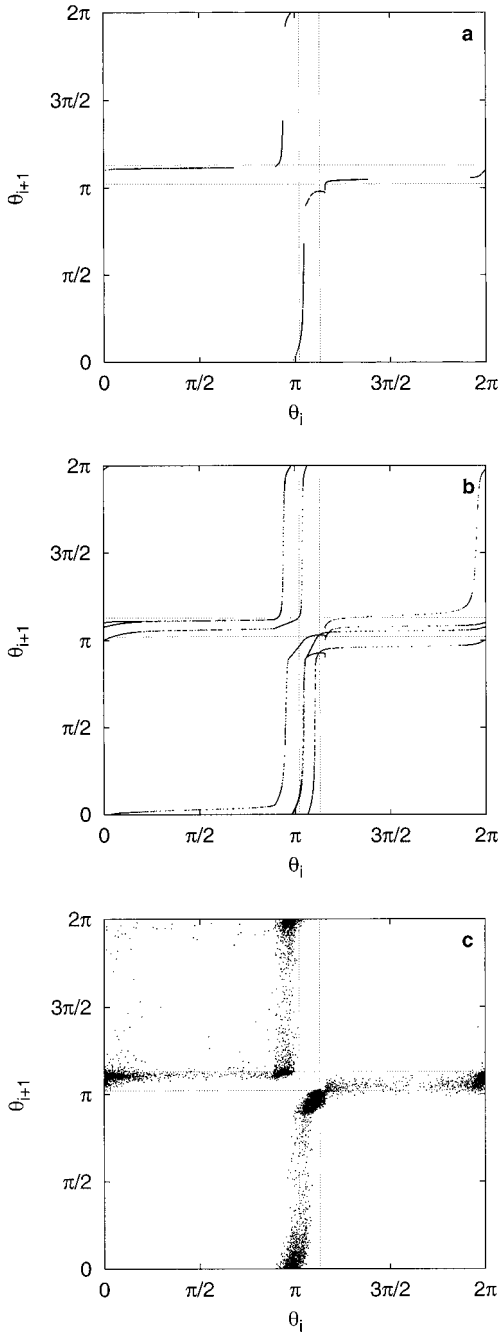

Figure 15. Return maps for (a) $\kappa = 0$, (b) $\kappa = 0.12$ with dichotomously varied switching times, and (c) $\kappa = 0.12$ for a system with Gaussian variability in its switching times. The parameters are set as those for system 1 in Figure 7. The dotted lines indicate the phase angle range corresponding to the boxed region in Figure 12.

amplitude, several things happen. First, the map becomes multivalued. In the dichotomous case (Figure 15b), the map consists of a series of curves due to the discrete nature of the noise process. In the Gaussian case (Figure 15c), simple spreading is observed. In addition, some of the gaps in the original map are filled in, indicating that switching occurs more uniformly over the attractor with noise than without. This results in an increase in the number of ways the system can reach the region favorable to synchronization. Finally, at sufficiently large noise amplitudes, trajectories can visit the synchronization region in two successive cycles (points in panels b and c in the central square). Such events, although rare, greatly enhance the rate at which the systems becomes synchronized.

Note that, although we have concentrated on the case of oscillatory-to-oscillatory switching in this section, the situation in the excitable to oscillatory case is qualitatively identical.

Discussion and Conclusions

In this study, we have shown the feasibility of synchronizing two chemical systems operating under slightly different conditions. This is an important demonstration because we can in general expect small quantitative differences between any two chemical reactors of similar design. Perfect phase synchronization can be achieved when the two driven systems are switched between two limit cycles or between excitable and oscillatory states. When there exist large differences between q_1 and q_2 or between ϵ_1 and ϵ_2, it becomes very difficult to find a periodic forcing regime in which both systems exhibit complex oscillations. We have checked the above results with other combinations of T_{+c} and T_{-c}, ϵ_1 and ϵ_2, and q_1 and q_2. Qualitatively, the same results are obtained. When random variations are added to the durations of the forcing, the noise strength κ is limited by the values of $\bar{T}_+$ and $\bar{T}_-$; that is, 2κ must be no larger than $\bar{T}_+$ or $\bar{T}_-$. In the case that $\bar{T}_-$ (or $\bar{T}_+$) is too small, perfect phase synchronization cannot be achieved because of this limitation of the noise strength. However, larger noise strengths can be used if we limit random variation to the larger of the two phases ($\bar{T}_+$ or $\bar{T}_-$). Synchronization can still be obtained if only one of the two durations is variable, as discussed elsewhere.[19]

We have also briefly studied the effect of additive noise in the rate equations to represent the inherent fluctuations in chemical reactors (e.g., fluctuations in pumping rates). These additive noise terms were generated independently for the two systems to be synchronized. We have found that the synchronization properties described in this paper are robust with respect to this additional source of stochasticity.

The phase difference between the two systems varies in time in the chaotic region, whereas it remains constant in the nonchaotic region. We find that the noise strength has to be above a threshold to obtain perfect phase synchronization, suggesting that shifting the two systems out of the chaotic region plays an important role here. For Gaussian-distributed noise, the noise process can generate a sequence of small numbers. When this happens, the two driven systems will return momentarily to the chaotic region. The sensitive dependence property of chaos will then cause a loss of synchronization until larger fluctuations shift the two systems out of the chaotic region again. This in part explains why dichotomous noise of smaller strength than in the Gaussian case can be used to achieve phase synchronization.

Noise-induced transitions between attractors have been observed in a number of contexts.[60−65] In our study, the rate of transitions between a synchronized and an unsynchronized (or simply lag-synchronized) state can be controlled through the statistical properties of the fluctuations (noise strength, correlation, etc.). Higher noise strengths tend to favor synchronization, whereas correlated noise processes generally enhance the transition rate. Noise-induced transitions can sometimes be exploited for practical purposes. For instance, Hasty and coworkers have demonstrated that bistable genetic networks can be switched between on and off states by short noise pulses.[65]

It has been suggested[11,24] that perfect phase synchronization cannot be achieved among periodically driven chaotic systems because the phases in those systems are not free. This study, together with earlier studies,[1,19] suggests that the introduction of random variation in the duration of the periodic forcing can overcome the above problem to eventually build up phase synchronization among (nearly) periodically driven systems. Noise-induced coherent motion has been observed in a variety of studies.[16,17,56] This contribution further demonstrates the constructive role which can be played by noise. The results also illustrate that adding random variability to the *duration* of the forcing phases is a powerful complement to the traditional way of perturbing the *intensity* of external forcing, in particular when the intensity can only be varied within a narrow range. The above results also indicate that dichotomous noise is more effective than Gaussian distributed noise in obtaining a synchronized state because it requires smaller noise strength for successful synchronization.

The explanation of the synchronization mechanism presented in section 3.4 is incomplete. After attempting many other styles of explanation however, we have come to the conclusion that explanations of synchronization in randomly switched systems require an analysis of the behavior in phase space, either directly[1] or in a suitably constructed Poincaré map, as we have done here. The Poincaré maps of Figure 15 reduce the dynamics to a circle map, suggesting that further insight might be obtained by seeking similar phenomena in analytic circle maps such as the sine map,[66] an avenue of investigation which we are currently pursuing.

Acknowledgment. We thank the anonymous referees whose suggestions and questions led to substantial improvements in this paper. We are also grateful to Ms. Arlene Nelson for drawing Figure 1. This work was supported by the Natural Sciences and Engineering Research Council of Canada.

References and Notes

(1) Closson, T. L. L.; Roussel, M. R. *Phys. Rev. Lett.* **2000**, *85*, 3974.
(2) Elson, R. C.; Selverston, A. I.; Huerta, R.; Rulkov, N. F. *Phys. Rev. Lett.* **1998**, *81*, 5692.
(3) Goodwin, B. C. *Eur. J. Biochem.* **1969**, *10*, 511.
(4) Carroll, T. L. *Biol. Cybern.* **1995**, *73*, 553.
(5) Feng, J.; Brown, D.; Li, G. *Phys. Rev. E* **2000**, *61*, 2987.
(6) Blasius, B.; Huppert, A.; Stone, L. *Nature* **1999**, *399*, 354.
(7) Neiman, A.; Schimansky-Geier, L.; Cornell-Bell, A.; Moss, F. *Phys. Rev. Lett.* **1999**, *83*, 4896.
(8) Fitzgerald, R. *Phys. Today* March, **1999**, 18.
(9) Tass, P.; Rosenblum, M. G.; Weule, J.; Kurths, J.; Pikovsky, A.; Volkmann, J.; Schnitzler, A.; Freund, H.-J. *Phys. Rev. Lett.* **1998**, *81*, 3291.
(10) Jouaville, L. S.; Ichas, F.; Holmuhamedov, E. L.; Camacho, P.; Lechleiter, J. D. *Nature* **1995**, *377*, 438.
(11) Rosenblum, M. G.; Pikovsky, A. S.; Kurths, J. *Phys. Rev. Lett.* **1996**, *76*, 1804.
(12) Xiao, J. H.; Hu, G.; Qu, Z. *Phys. Rev. Lett.* **1996**, *77*, 4162.
(13) Pikovskii, A. S. *Radiophys. Quantum Electron.* **1984**, *27*, 390.
(14) Pikovsky, A. S.; Rosenblum, M. G.; Osipov, G. V.; Kurths, J. *Physica D* **1997**, 219.
(15) Park, E.-H.; Zaks, M. A.; Kurths, J. *Phys. Rev. E* **1999**, *60*, 6627.
(16) Hu, B.; Zhou, C. *Phys. Rev. E* **2000**, *61*, R1001.
(17) Neiman, A.; Schimansky-Geier, L.; Moss, F.; Shulgin, B.; Collins, J. *Phys. Rev. E* **1999**, *60*, 284.
(18) Parmananda, P.; Jiang, Y. *J. Phys. Chem. A* **1998**, *102*, 4532.
(19) Roussel, M. R.; Wang, J. *J. Phys. Chem. A* **2000**, *104*, 11751.
(20) Blekhman, I. I. *Synchronization in Science and Technology*; ASME Press: New York, 1988.
(21) Pecora, L. M.; Carroll, T. L. *Phys. Rev. Lett.* **1990**, *64*, 821.
(22) Sun, H.; Scott, S.; Showalter, K. *Phys. Rev. E.* **1999**, *60*, 3876.
(23) Josic, K. *Phys. Rev. Lett.* **1998**, *80*, 3053.
(24) Zaks, M. A.; Park, E.-H.; Rosenblum, M. G.; Kurths, J. *Phys. Rev. Lett.* **1999**, *82*, 4228.
(25) Brown, R.; Kocarev, L. *Chaos* **2000**, *10*, 344.
(26) Bailey, J. E. *Chem. Eng. Commun.* **1973**, *1*, 111.
(27) Sincic, D.; Bailey, J. E. *Chem. Eng. Sci.* **1977**, *32*, 281.
(28) Cordonier, G. A.; Schmidt, L. D.; Aris, R. *Chem. Eng. Sci.* **1990**, *45*, 1659.
(29) Boiteux, A.; Goldbeter, A.; Hess, B. *Proc. Natl. Acad. Sci. U.S.A.* **1975**, *72*, 3829.
(30) Daido, H.; Tomita, K. *Prog. Theor. Phys.* **1979**, *61*, 825.
(31) Daido, H.; Tomita, K. *Prog. Theor. Phys.* **1979**, *62*, 1519.

(32) Kai, T.; Tomita, K. *Prog. Theor. Phys.* **1979**, *61*, 54.
(33) Mankin, J. C.; Hudson, J. L. *Chem. Eng. Sci.* **1984**, *39*, 1807.
(34) Kevrekidis, I. G.; Schmidt, L. D.; Aris, R. *Chem. Eng. Commun.* **1984**, *30*, 323.
(35) Kevrekidis, I. G.; Schmidt, L. D.; Aris, R. *Chem. Eng. Sci.* **1986**, *41*, 1263.
(36) Kevrekidis, I. G.; Aris, R.; Schmidt, L. D. *Chem. Eng. Sci.* **1986**, *41*, 905.
(37) McKarnin, M. A.; Schmidt, L. D.; Aris, R. *Chem. Eng. Sci.* **1988**, *43*, 2833.
(38) Vance, W.; Ross, J. *J. Chem. Phys.* **1989**, *91*, 7654.
(39) Schreiber, I.; Dolník, M.; Choc, P.; Marek M. *Phys. Lett. A* **1988**, *128*, 66.
(40) Dolník, M.; Finkeová, J.; Schreiber, I.; Marek, M. *J. Phys. Chem.* **1989**, *93*, 2764.
(41) Scott, S. K. *Chemical Chaos*; Oxford University Press: Oxford, U.K., 1991.
(42) Förster, A.; Hauck, T.; Schneider, F. W. *J. Phys. Chem.* **1994**, *98*, 184.
(43) Schneider, F. W. *Annu. Rev. Phys. Chem.* **1985**, *36*, 347.
(44) Aronson, D. G.; McGehee, R. P.; Kevrekidis, I. G.; Aris, R. *Phys. Rev. A* **1986**, *33*, 2190.
(45) Hohmann, W.; Lebender, D.; Müller, J.; Schinor, N.; Schneider, F. W. *J. Phys. Chem. A* **1997**, *101*, 9132.
(46) Field, R. J.; Noyes, R. M. *J. Chem. Phys.* **1974**, *60*, 1877.
(47) Kuhnert, L.; Agladze, K. I.; Krinsky, V. I. *Nature* **1989**, *337*, 244.
(48) Krug, H.-J.; Pohlmann, L.; Kuhnert, L. *J. Phys. Chem.* **1990**, *94*, 4862.
(49) Tyson, J. J.; Fife, P. C. *J. Chem. Phys.* **1980**, *73*, 2224.
(50) Sørensen, P. G.; Lorenzen, T.; Hynne, F. *J. Phys. Chem.* **1996**, *100*, 19192.
(51) Kádár, S.; Amemiya, T.; Showalter, K. *J. Phys. Chem.* **1997**, *101*, 8200.
(52) Hanazaki, I.; Mori, Y.; Sekiguchi, T.; Rabai, G. *Physica D* **1995**, *84*, 228.
(53) Ram Reddy, M. K.; Szlávik, Z.; Nagy-Ungvarai, Zs.; Müller, S. C. *J. Phys. Chem.* **1995**, *99*, 15081.
(54) Agladze, K.; Obata, S.; Yoshikawa, K. *Physica D* **1995**, *84*, 238.
(55) Yamaguchi, T.; Shimamoto, Y.; Amemiya, T.; Yoshimoto, M.; Ohmori, T.; Nakaiwa, M.; Akiya, T.; Sato, M.; Matsumura-Inoue, T. *Chem. Phys. Lett.* **1996**, *259*, 219.
(56) Irwin, A. J.; Fraser, S. J.; Kapral, R. *Phys. Rev. Lett.* **1990**, *64*, 2343.
(57) Steinmetz, C. G.; Larter, R. *J. Chem. Phys.* **1991**, *94*, 1388.
(58) Rangarajan, G.; Habib, S.; Ryne, R. D. *Phys. Rev. Lett.* **1998**, *80*, 3747.
(59) van Kampen, N. G. *Stochastic Processes in Physics and Chemistry*; North-Holland: Amsterdam, 1987; pp 94−98.
(60) L'Heureux, I.; Kapral, R.; Bar-Eli, K. *J. Chem. Phys.* **1989**, *91*, 4285.
(61) Guillouzic, S.; L'Heureux, I. *Phys. Rev. E* **1997**, *55*, 5060.
(62) Liu, J.; Crawford, J. W. *Biophys. Chem.* **1997**, *69*, 97.
(63) Lapidus, L. J.; Enzer, D.; Gabrielse, G. *Phys. Rev. Lett.* **1999**, *83*, 899.
(64) Milstein, G. N.; Tretyakov, M. V. *Physica D* **2000**, *140*, 244.
(65) Hasty, J.; Pradines, J.; Dolnik, M.; Collins, J. J. *Proc. Natl. Acad. Sci. U.S.A.* **2000**, *97*, 2075.
(66) Ecke, R. E.; Farmer, J. D.; Umberger, D. K. *Nonlinearity* **1989**, *2*, 175.